UNITED NATIONS EDUCATIONAL, SCIENTIFIC AND CULTURAL ORGANIZATION
INTERNATIONAL ATOMIC ENERGY AGENCY
INTERNATIONAL CENTRE FOR THEORETICAL PHYSICS

SMR/917 - 4

SECOND WORKSHOP ON SCIENCE AND TECHNOLOGY OF THIN FILMS

(11 - 29 March 1996)

Reading material about:
" Nanomagnetic properties of thin films "

presented by:

R. WIESENDANGER
Universität Hamburg
Institut für Angewandte Physik
Jungiusstrasse 11
D-20355 Hamburg
Germany

Bubble domains in garnet films studied by magnetic force microscopy

A. Wadas[a] and R. Wiesendanger
Institute of Applied Physics, University of Hamburg, 20355 Hamburg, Germany

P. Novotny
Institute of Chemical Technology, 166 28 Prague 6, Czech Republic

(Received 30 March 1995; accepted for publication 9 August 1995)

We have studied magnetic domain structure in $(YSmLuCa)_3(FeGe)_5O_{12}$ garnet thin film by using magnetic force microscopy (MFM). Domain wall contrast of bubble domains has been revealed using Permalloy–Fe double-layer thin-film tips. We have also observed that nanometer scale deformations of the surface disturb a magnetic bubble structure by introducing stripe domains. MFM images have shown that stripe domains pin their domain walls to surface scratches. The domains can change their location with respect to a scratch by switching a domain wall pinned to a scratch. © *1995 American Institute of Physics.*

Development of vertical Bloch line (VBL) memories in garnet films requires among many others also good observability of domain wall structures.[1] Domains and domain walls are usually observed by means of optical methods.[2,3] Partial grooving of bubble garnets, necessary to stabilize stripe and bubble domains, is the other factor required to control a good performance of VBL memories.[4–6] The topography of the surface has to be then precisely defined. The two important features, domain wall contrast and the topography of the same area, can be simultaneously measured with magnetic force microscopy (MFM). Using MFM we have found that scratches of a depth of few nanometers disturb a bubble structure in magnetic garnet film by introducing stripe domains. This opens the possibility of modifying the domain structure by nanometer scale surface deformation.

In this communication, we present the first result obtained on bubble domains in magnetic garnet films with magnetic force microscopy (MFM). MFM is the method which relies on the magnetostatic interaction between the magnetic sample and the magnetic sensor (tip) attached to a cantilever placed tens of nanometers over the sample.[7] Scanning the sample at a specific height, we have monitored the deflection of the cantilever due to magnetic tip–sample interaction. This has provided a map of forces sensed over the sample. The magnetic force exerted on the tip is the convolution of the sample field gradient and the tip magnetization over the volume of the tip.[8]

dc operation of MFM, as we have previously described, gives the opportunity to acquire magnetic and corresponding topographic images of the same area simultaneously.[9,10] This is an important advantage over optical methods used to study domain walls. The most difficult task necessary to solve has been to establish the reliable and most sensitive magnetic sensor able to reflect the domain wall structure. We have previously found that the iron thin films deposited on commercially available Si_3N_4 pyramidal tips form magnetically sensitive tips which are able to obtain domain wall contrast on a stripe domain structure in magnetic garnet.[9] However, a similar single-layer magnetic thin-film tip has not given well-reproducible domain wall contrast on bubble domains. The problem with a single-layer thin-film tip has been its too high coercivity and small signal-to-noise ratio.

These remarks are valid with respect to MFM data obtained on bubble domains. In order to overcome these difficulties, mainly to decrease the coercive force H_c of magnetic tips, we have used laminated tips.[10] Laminated magnetic films deposited on flat surfaces have been studied for many years.[10–15] Among other features it was found that laminated 80–20 nickel–iron films exhibit about ten times lower coercive force than a single layer of the same thickness. Similar H_c reduction was also observed in double films.[12,13] According to the theory the reduction of H_c is related to a reduction of the energy of walls in such double films.[16] Small thickness of a spacer helps to form ferromagnetic microbridges which might influence the interaction between magnetic layers.[17] Since Si_3N_4 tips have pyramidal shapes we did not have the same deposition conditions as for previously studied laminated films. After testing different compositions of laminated tips we have achieved the best MFM images with Permalloy–Fe double films separated by 3 nm of Au. The thickness of the Permalloy layer has been in the range from 12 to 18 nm. The second magnetic layer, Fe, has been deposited with a thickness of 10–15 nm. We have also used Cr as a spacer between magnetic layers. Usually the signal-to-noise ratio in MFM data obtained with these tips is slightly lower than with Au spacer. The last layer evaporated on the magnetic double-film tip against oxidation and mechanical wear has been thin layer of 10 nm of Au. Tips were not magnetized prior to the experiment.

We have studied an epitaxially grown $(YSmLuCa)_3(FeGe)_5O_{12}$ garnet film on $Gd_3Ga_5O_{12}$ substrate. The garnet film has a thickness of 4.7 μm and a quality factor $Q=2.5$. The bubble structure has been obtained by applying a nearly in-plane constant magnetic field.

Figure 1 is an example of MFM data obtained with a tip that was coated with 12 nm of Permalloy, 3 nm of Au as a spacer, and 10 nm of Fe as a second layer. It shows a 15×15 μm^2 scan. The nominal tip–sample separation was 100 nm for this image. The bright rings represent the domain wall contrast in the bubble garnet film. The diameter of a bubble domain is about 3 μm. Having a magnetically soft tip we

[a]Electronic mail: wadas@physnet.uni-hamburg.de

 0021-8979/95/78(10)/6324/3/$6.00

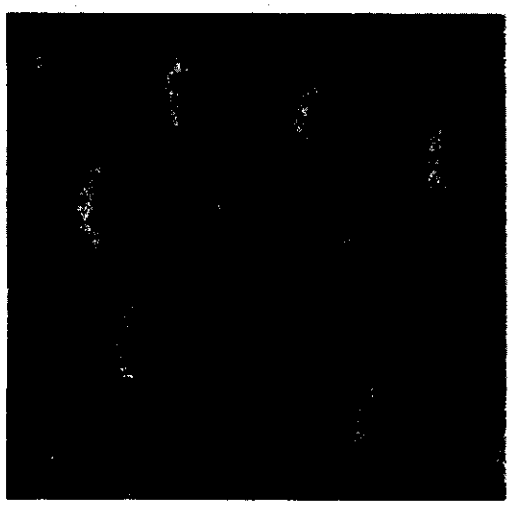

FIG. 1. Magnetic bubble domain structure of a garnet film obtained with a Permalloy–Fe thin-film tip. Bright rings represent domain wall contrast. The tip–sample separation was 100 nm.

expect that the tip has been always attracted over the domains regardless of the domain polarization, when the coercive force of the tip is smaller than the stray field arising from the domains. We have observed lower (attraction) contrast over the domains and higher (bright rings) due to domain walls.

In Fig. 2 we show an example of the direct dependence of the domain structure on a surface deformation. The MFM image is in Fig. 2(a). The lower part of Fig. 2 is a topographic image with a scratch with a width of 440 nm and depth of 11 nm. Exactly along the scratch lies the stripe domain. The bright line which encircles the domain represents the domain wall contrast. Two rows of bubble domains arrange themselves along the stripe domain as pinned to the stripe. Although surface grooving is a common method to stabilize stripe and bubble domains a relation between a domain structure and surface deformation on nanometer scale is still not known in detail.[2,5] Thorough inspection of Fig. 2 and other images (not shown because of space) reveals that a domain wall of the stripe domain sits exactly at the position of a scratch. If a domain wall is in the middle of the scratch, then the magnetic charges induced on opposite side surfaces have different signs and thus the scratch serves as a minisource of an inhomogenous magnetic field. The surface density of a magnetic charge is described by $M(\alpha-\beta)$ where M is the magnetization of the garnet, β is the angle between magnetization M and the easy axis (z), and α denotes the slope of the side of the scratch.

According to our knowledge such an effect of a nanometer scale surface deformation on a bubble magnetic structure has not yet been reported. This direct correlation between a

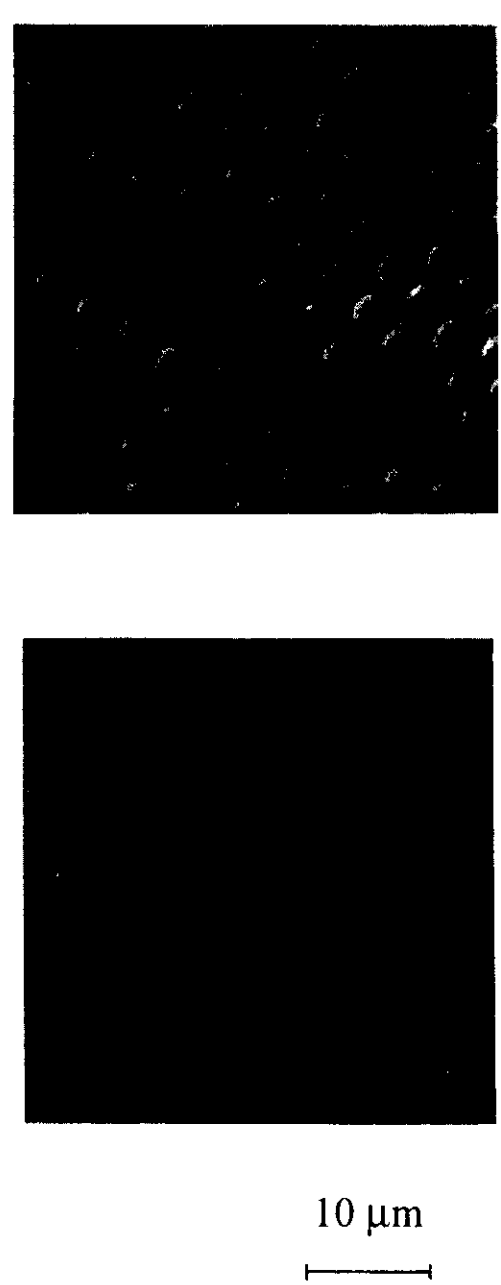

FIG. 2. The upper part is a magnetic bubble structure with a stripe domain observed by MFM. The topographic image of the same area with a scratch which generated the stripe domain is below the MFM image. One of the domain walls of the stripe domain is pinned to the scratch.

domain structure and a nanometer scale modification of the surface is a very important effect which might be used in magnetic recording.

As we have mentioned at the beginning of this communication we did not magnetize MFM tips before an experiment. According to our experience, magnetizing the tip usually leads to MFM image without domain wall contrast, for example shown in Fig. 3(a). Then the tip was magnetized perpendicular to the sample surface. The MFM image shows a very weak domain wall contrast but quite a strong domain contrast. The bubble domains appear as white circles. There are also two stripe domains pinned to narrow scratches visible in the topographic image [Fig. 3(b)] with a width of 400

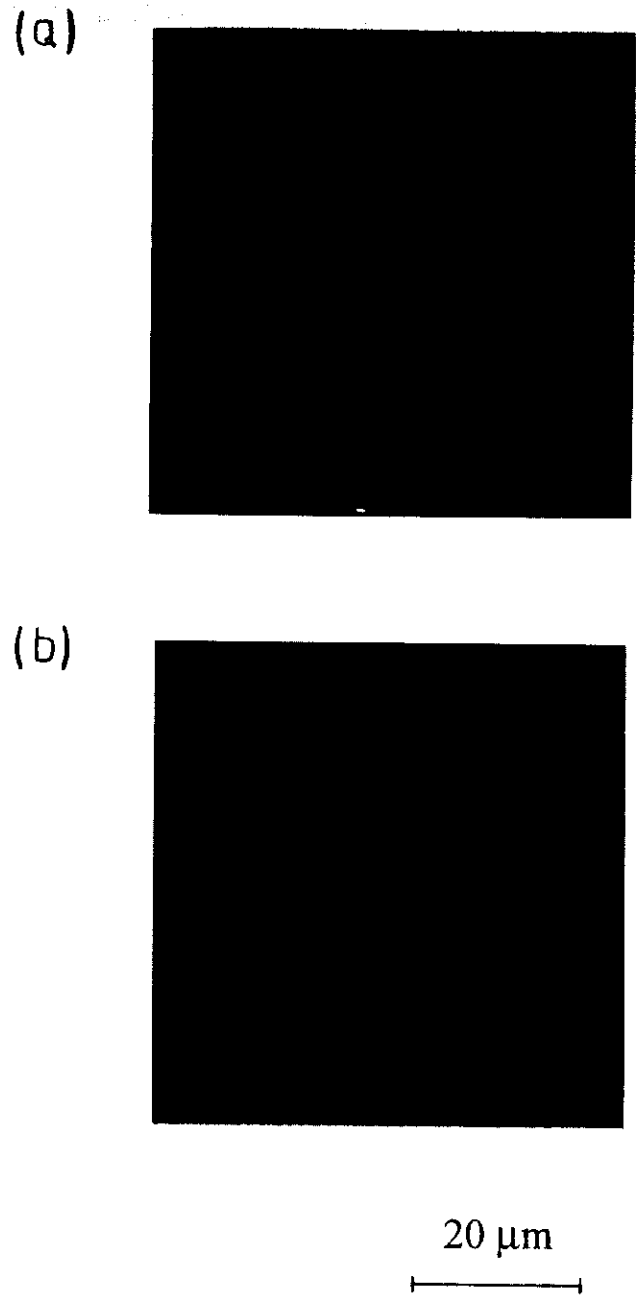

FIG. 3. Magnetic bubble structure observed by MFM with a magnetized tip. There are no rings but only circles. One of the stripe domains changes its position with respect to the scratch by switching the pinned domain wall. Two parallel scratches are visible on the topographic image.

nm and a depth of 10 nm. One of these stripe domains switches its position on the scratch sitting on it first with one domain wall pinned to the scratch and then with the other one.

It is also important to notice that at the left-hand-side upper corner of the MFM image some bubble domains harbored to the scratch are flattened. This might be the primary and necessary status before they build up a stripe domain. Two of these domains are already connected with each other. They form a new stripe domain which will lie along on both sides of the scratch if a process of building up proceeds in the opposite directions.

In summary, we have used MFM to study bubble domains on garnet film. Using Permalloy–Fe double thin-film tips we have imaged walls of bubble domains. Simultaneously acquiring MFM images and topographic scans has given us an opportunity to investigate the direct dependence of magnetic domain structure on surface morphology. Furthermore, we have observed that nanometer-deep scratches on the surface have caused significant changes in a bubble domain structure.

Comparing MFM data with the corresponding topographic scan we have found that stripe domains pin their domain walls to surface scratches. These correlations between topography and magnetic structure open the possibility to introduce and manipulate stripe domains within bubble structure by controlled surface modification on a nanometer scale.

A.W. would like to thank Shuheng Pan for many discussions of different aspects of this work.

[1] S. Konishi, IEEE Trans. Magn. **MAG-19**, 1838 (1983).
[2] H. Matsutera, K. Mizuno, and Y. Hidaka, IEEE Trans. Magn. **MAG-23**, 2320 (1987).
[3] A. Thiaville, F. Boileau, J. Miltat, and L. Arnaud, J. Appl. Phys. **63**, 3153 (1988).
[4] J. C. Wu, R. R. Katti, and H. L. Stadler, IEEE Trans. Magn. **MAG-28**, 2338 (1992).
[5] T. Suzuki, K. Matsuyama, H. Asada, and S. Konishi, IEEE Trans. Magn. **MAG-23**, 3393 (1987).
[6] J. C. Wu, R. R. Katti, and H. L. Stadler, J. Appl. Phys. **69**, 5751 (1991).
[7] Y. Martin and H. K. Wickramasinghe, Appl. Phys. Lett. **50**, 1455 (1987).
[8] A. Wadas and P. Grütter, Phys. Rev. B **39**, 12 013 (1989).
[9] A. Wadas, J. Moreland, P. Rice, and R. R. Katti, Appl. Phys. Lett. **64**, 1156 (1994).
[10] A. Wadas, P. Rice, and J. Moreland, Appl. Phys. A **59**, 63 (1994).
[11] H. Clow, Nature **194**, 1035 (1962).
[12] S. Middelhoek and Z. Angew, Phys. **18**, 524 (1965) (in English).
[13] F. J. Friedländer and L. F. Silva, J. Appl. Phys. **36**, 946 (1965).
[14] O. Massenet, F. Biragnet, H. Juretschke, R. Montmory, and A. Yelon, IEEE Trans. Magn. **553** (1966).
[15] E. Feldtkeller, J. Appl. Phys. **39**, 1181 (1968).
[16] J. C. Slonczewski and S. Middelhoek, Appl. Phys. Lett. **6**, 139 (1965).
[17] H. J. Juretschke, Bull. Am. Phys. Soc. **11**, 110 (1966).

Observation of Vacuum Tunneling of Spin-Polarized Electrons with the Scanning Tunneling Microscope

R. Wiesendanger and H.-J. Güntherodt
Institute of Physics, University of Basel, Klingelbergstrasse 82, CH-4056 Basel, Switzerland

G. Güntherodt
II. Institute of Physics, Rheinisch-Westfälische Technische Hochschule Aachen, D-5100 Aachen, Federal Republic Germany

R. J. Gambino and R. Ruf
IBM T. J. Watson Research Center, Yorktown Heights, New York 10598
(Received 27 March 1990)

Vacuum tunneling of spin-polarized electrons from a ferromagnetic CrO_2 tip into a Cr(001) single crystal has been observed by means of a scanning tunneling microscope (STM) operated in UHV. Topographic STM images of the Cr(001) surface using a tungsten tip confirm the model of topological antiferromagnetism between ferromagnetic terraces separated by monatomic steps of 0.144-nm height. With CrO_2 tips, the measured step-height values alternate around the mean value of 0.144 nm due to an additional contribution from spin-polarized-electron tunneling.

PACS numbers: 75.30.Pd, 61.16.Di, 75.25.+z, 75.50.Ee

Over the past two decades, a number of experimental techniques has been developed to investigate surface magnetism, such as spin-polarized (SP) field emission, SP photoemission, SP tunneling, electron-capture spectroscopy, SP-LEED, Lorentz microscopy, scanning electron microscopy with polarization analysis (SEMPA), and, more recently, magnetic force microscopy (MFM).[1] These techniques can be used, for instance, to measure the spin polarization averaged over surface regions determined by the spatial extension of the probe, to investigate magnetic domain structures, and to probe spin-dependent energy states. Although some of the above-mentioned experimental techniques, such as SEMPA or MFM, simultaneously offer a high spatial resolution of the order of 10 nm, an experimental tool probing real-space magnetic structures down to the atomic scale has not been demonstrated. Since the invention of scanning tunneling microscopy[2] (STM), which allows the determination of real-space atomic structures, the question arose whether this technique can also be made sensitive to the electron spin and therefore to magnetic structures on the atomic scale. It has already been shown that SP secondary electrons, generated by STM in the field-emission mode, may be used in the future for magnetic imaging on a nanometer scale[3] and that a direct observation of the precession of individual paramagnetic spins on oxidized silicon surfaces is possible by STM.[4] However, evidence has not yet been obtained for tunneling of SP electrons in a STM experiment, offering the opportunity to investigate real-space magnetic structures down to the atomic scale. In contrast to SP tunneling studies using planar tunneling junctions, which can either be superconductor-oxide-ferromagnet junctions[5] or ferromagnet-oxide-ferromagnet junctions,[6] the STM technique promises to allow the determination of the local spin polarization. Here, we report on the first vacuum tunneling experiments of SP electrons from ferromagnetic CrO_2 tips into a Cr(001) surface by means of a STM. We first show that topographic STM measurements performed with a tungsten tip on the Cr(001) surface support the microscopic model by Blügel, Pescia, and Dederichs[7] of topological antiferromagnetism between ferromagnetic terraces separated by single steps. After replacing the tungsten tip by a ferromagnetic CrO_2 tip, a characteristic alternation of the measured monatomic step-height values is observed which we attribute to an additional contribution from SP tunneling. An expression is derived relating the spin polarization with quantities directly measurable with the STM.

The experiments were performed in a multichamber UHV system (Nanolab) with several surface preparation and analysis facilities.[8] The pressure in the STM chamber was 1×10^{-11} mbar during all the STM studies reported in this Letter. The calibration of the STM scanning unit was performed laterally by imaging the Si(111)-7×7 (Ref. 9) and the Si(001)-2×1 (Ref. 10) surface structures and perpendicular to the surface by imaging monatomic steps on the Si(001)-2×1 surface. It is important for our analysis of the step structure of the Cr(001) surface that a clear distinction between monatomic and biatomic steps can be made by comparing with the step-height values found on the Si(001)-2×1 surface. On this surface, monatomic steps separate terraces with the dimer rows oriented at 90° relative to each other, whereas a parallel orientation of the dimer rows is observed on terraces separated by biatomic steps. The noise level of the STM instrument is well below 0.01 nm, which has been proved by imaging the atomic structure of the hexagonally close-packed Au(111) surface with a measured corrugation of the order of 0.02 nm.[8]

All STM data presented in this Letter represent raw data.

For comparison of STM studies with nonmagnetic and magnetic probes, we used electrochemically etched tungsten tips and ferromagnetic CrO_2 tips, respectively. These CrO_2 tips were obtained by first growing 1-μm-thick CrO_2 films with in-plane magnetization on Si(111) substrates covered with a 35-nm-thick TiO_2 nucleation layer. The CrO_2 was deposited by decomposing CrO_3 vapor on a heated substrate in a convection reactor operated in ambient air. The Si(111) substrates were scribed and cleaved on (111) planes after the deposition of the CrO_2 films. The cleavage cracks propagate through the brittle CrO_2 film to give a tip shape at the intersection of particular cleavage planes. The Si substrate at the front end of each tip is etched back in HF-HNO_3 solution which preferentially dissolves the silicon. The overhanging CrO_2 film is used as a magnetic probe. The films have a large remanent magnetization ($\sim$90% of saturation) so the tip is likely to be in a single domain, saturated state. The in-plane magnetization of the CrO_2 films together with the shape anisotropy of the tip lead to a preferred magnetization direction perpendicular to the sample surface in the STM experiment. Recent spin-resolved photoemission experiments on similar ferromagnetic CrO_2 films showed a spin polarization of nearly 100% for binding energies near 2 eV below the Fermi level E_F.[11] The large value of the spin polarization may be explained by a spin-filter effect of CrO_2 as a conjectured half-metallic ferromagnet[12] or a more semiconductorlike ferromagnet.[11] The CrO_2 tips were therefore favored for SP tunneling experiments with the STM, although they could not so far be prepared as sharp as electrochemically etched tungsten tips.

Apart from the problem of choosing the appropriate SP electron source, a magnetic test structure was needed. We have chosen the Cr(001) surface for the following reason. Recently, Blügel, Pescia, and Dederichs[7] showed on the basis of self-consistent total-energy calculations that topological antiferromagnetism between ferromagnetic terraces separated by single steps (Fig. 1) is the energetically most favorable structure of this surface. This topological antiferromagnetism of the Cr(001) surface is compatible with both the absence of magnetization observed by spin-resolved photoemission[13] which arises from the cancellation between oppositely magnetized terraces within the diameter of the light spot, as well as with the existence of spin-split surface states detected by energy- and angle-resolved photoemission[14] which are due to majority- and minority-spin states inside each ferromagnetic terrace. The topological antiferromagnetism of the Cr(001) surface with terraces alternately magnetized in opposite directions provides an ideal test structure for SP-STM experiments.

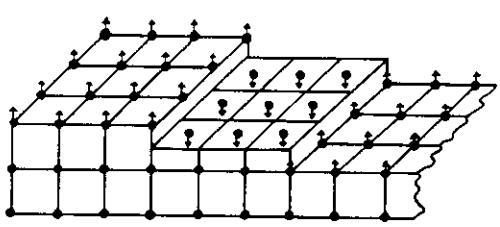

FIG. 1. Topological antiferromagnetic order of the Cr(001) surface with terraces separated by monatomic steps. Different terraces are magnetized in opposite directions. Only surface spins are indicated. (Figure taken from Ref. 7.)

Our topographic STM studies of the Cr(001) surface also strongly support this microscopic model with terraces separated predominantly by monatomic steps [Fig.

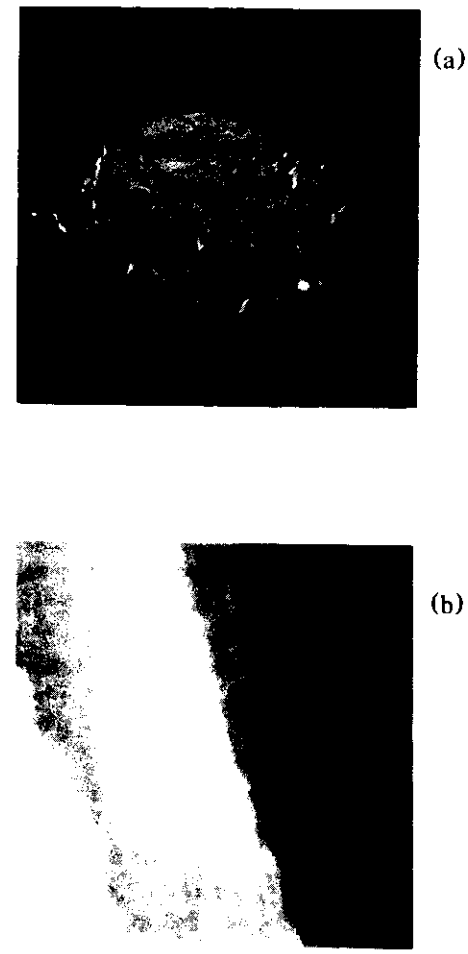

FIG. 2. (a) Constant-current STM image (perspective view) of the Cr(001) surface $(128\ \text{nm})^2$ obtained with a tungsten tip. Terraces separated predominantly by monatomic steps can be seen. A screw dislocation appears in the upper right-hand part of the image. (Tunneling current $I = 1$ nA, sample bias voltage $U = +0.05$ V.) (b) Constant-current STM image (top view) of the Cr(001) surface $(32\ \text{nm})^2$ obtained with a CrO_2 tip showing again terraces separated by monatomic steps with different gray levels for each terrace. (Tunneling current $I = 1$ nA, sample bias voltage $U = +2.5$ V.)

2(a)]. The mechanically and electrolytically polished Cr(001) surface was prepared *in situ* over a time period of several months by cycles of Ar^+-ion etching and annealing. A $p(1\times1)$ LEED pattern was obtained, characteristic of a clean Cr(001) surface.[14] Only small traces of oxygen and nitrogen could be detected by x-ray photoelectron spectroscopy. The average width and shape of the observed terraces were found to depend on the annealing conditions, whereas the preferred occurrence of monatomic steps was independent of the preparation conditions. The experimental determination of the monatomic step-height value yields 0.149 ± 0.008 nm, in good agreement with half of the cubic unit-cell height of 0.144 nm for bcc Cr.

After replacing the tungsten tip by a CrO_2 tip, the STM images of the Cr(001) surface showed qualitatively the same topographic structures, i.e., terraces separated by monatomic steps [Fig. 2(b)]. Surprisingly, these monatomic steps could still be imaged with a remarkably high spatial resolution, although the CrO_2 tips appear macroscopically rather blunt. However, we find two different experimental results with CrO_2 tips compared to tungsten tips.

First, a positive sample bias voltage of at least 2 V had to be applied in order to get a stable tunneling current of 1 nA. The I vs V characteristics, which were recorded to investigate the bias-voltage dependence in more detail, showed the typical appearance of semiconductor-vacuum-metal tunneling rather than that for metal-vacuum-metal tunneling. This observation is consistent with results from spin-resolved photoemission from similar CrO_2 films showing low intensity in the photoemission spectra near E_F.[11] We therefore operated the STM always in a regime of maximum spin polarization of the CrO_2, which is found at about 2 eV below E_F.[11]

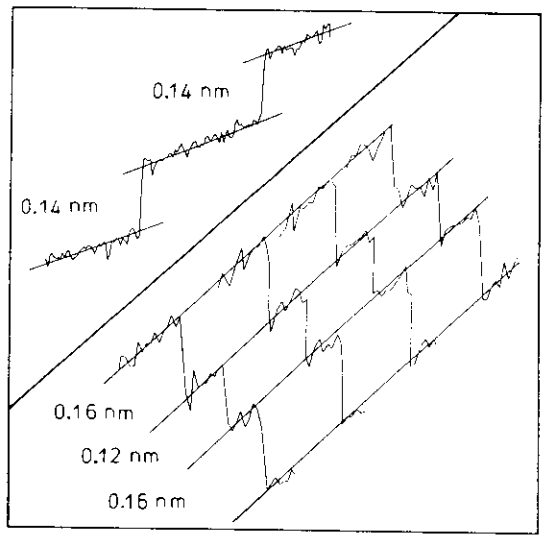

FIG. 3. Arbitrarily chosen (not successive) single-line scans over the same three monatomic steps taken from the STM image of Fig. 2(b), which was obtained with a CrO_2 tip. The same alternation of the step-height values (0.16, 0.12, and again 0.16 nm) in all single-line scans is evident. The line scans are 22 nm long. Inset: For comparison, a single-line scan over two monatomic steps taken from the STM image of Fig. 2(a), which was obtained with a tungsten tip. In this case, the measured step-height value is constant and corresponds to the topographic monatomic step height. This line scan is 70 nm long.

Second, a periodic alternation of the measured monatomic step heights between larger and smaller values compared to the mean single step-height value of 0.144 nm is observed (Fig. 3). To support this experimental result, we have analyzed the step heights from individual line scans of over twenty STM raw data images obtained in the constant-current mode. Care was taken to analyze only measured line scans (line scans in the x or y direction) and not oblique line scans where the exactness of the determination of the step-height values can suffer from the interpolation procedure necessary to get the topographic height values along these oblique line scans. It should be noted that the step-height values determined from topographic STM images might sometimes fluctuate within a few percent; however, a periodic alternation of the step-height values, as reproducibly observed in different line scans (independent measurements) with the CrO_2 tip on the Cr(001) surface, has never been found in topographic STM images measured with a tungsten tip. Furthermore, the deviation from the single step-height value determined with a CrO_2 tip can be as large as $\pm15\%$ which is outside the range of scatter of the monatomic step-height values measured with a tungsten tip. Therefore, we conclude that the observed periodic alternation of the single step-height values is characteristic for STM experiments performed with CrO_2 tips on a Cr(001) surface.

We interpret this periodic alternation of the monatomic step-height values as being due to an additional contribution from SP tunneling. Assume, as sketched in Fig. 4, that the CrO_2 tip is first scanning over a terrace having the same direction of magnetization as the front part

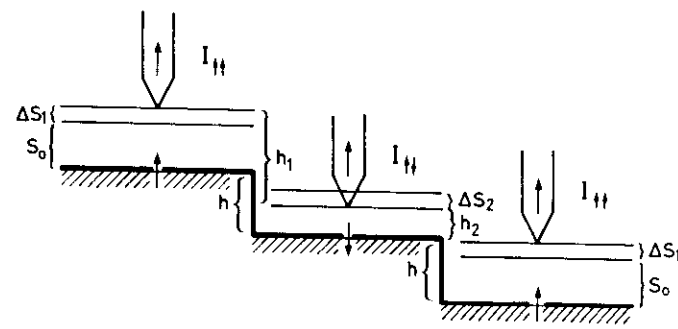

FIG. 4. Schematic drawing of a ferromagnetic tip scanning over alternately magnetized terraces separated by monatomic steps of height h. An additional contribution from SP tunneling leads to alternating step heights $h_1=h+\Delta s_1+\Delta s_2$ and $h_2=h-\Delta s_1-\Delta s_2$.

of the CrO_2 tip. The tunneling current $I_{\uparrow\uparrow}$ will then be increased due to a contribution from SP tunneling:[6]

$$I_{\uparrow\uparrow} = I_0(1+P), \tag{1}$$

where I_0 would be the tunneling current without this contribution and P is the effective spin polarization of our tunneling junction. Since the STM is operated at constant current, an additional contribution to the tunneling current leads to a corresponding increase Δs_1 of the mean distance s_0 between the tip and the sample surface. If the CrO_2 tip is scanning over a terrace having the opposite direction of magnetization, the tunneling current $I_{\uparrow\downarrow}$ will be decreased:

$$I_{\uparrow\downarrow} = I_0(1-P), \tag{2}$$

leading to a corresponding decrease Δs_2 of the distance between tip and sample. The measured single step-height values therefore alternate between $h_1 = h + \Delta s_1 + \Delta s_2$ and $h_2 = h - \Delta s_1 - \Delta s_2$, where h is the topographic monatomic step height. The relationship between

$$P = \frac{I_{\uparrow\uparrow} - I_{\uparrow\downarrow}}{I_{\uparrow\uparrow} + I_{\uparrow\downarrow}} \tag{3}$$

and $\Delta s_1, \Delta s_2$ is given by

$$P = \frac{\exp(A\sqrt{\phi}\Delta s_1) - \exp(-A\sqrt{\phi}\Delta s_2)}{\exp(A\sqrt{\phi}\Delta s_1) + \exp(-A\sqrt{\phi}\Delta s_2)} = \frac{\exp(A\sqrt{\phi}\Delta s) - 1}{\exp(A\sqrt{\phi}\Delta s) + 1}, \tag{4}$$

where ϕ is the mean local tunneling barrier height, $\Delta s = -\Delta s_1 + \Delta s_2$, and $A \approx 1\ \mathrm{eV}^{-1/2}\,\text{Å}^{-1}$. Equation (4) represents a relationship between the effective spin polarization P and the quantities ϕ and Δs which are directly measurable with the STM. Apart from the determination of the changes of the single step-height value, measurements of ϕ are necessary to derive P. We have determined ϕ from the slope of local $\ln I$ vs s characteristics. The value of ϕ lies between 3 and 5 eV for all of over one hundred $\ln I$ vs s characteristics which were measured with different sample bias voltages between +2.5 and +3.5 V. These ϕ values indicate that clean conditions for the tip and the sample surface were achieved, whereas anomalous low ϕ values were reported for contaminated surfaces of either tip or sample.[15] Therefore, we have confidence that the derived values for the polarization P cannot greatly be affected by surface contamination. Taking $\Delta s = 0.02 \pm 0.01$ nm and an average value of 4 ± 0.5 eV for ϕ, we derive values for P of $(20 \pm 10)\%$. The tip-to-sample distance at 1-nA tunneling current and a sample bias voltage of +2.5 V was determined to be about 0.5 nm. Measuring the distance and the bias-voltage dependence of the local spin polarization will both be interesting topics for future investigations.

In summary, we have demonstrated that SP tunneling can be detected and the local spin polarization P can be determined by the STM using ferromagnetic CrO_2 tips. This opens the door for studies of magnetic structures on the atomic scale by STM. Improvements in the sharpness of the ferromagnetic probing tips might lead, for instance, to the first real-space images of in-plane antiferromagnetic structures in the future.

We would like to thank Professor H. Thomas for many stimulating discussions, Professor A. Hubert for electropolishing the Cr(001) single crystal, D. Bürgler and G. Tarrach for their assistance and comments on the manuscript, as well as H. Breitenstein, H. R. Hidber, P. Reimann, R. Schnyder, and A. Tonin for their technical help. Financial support from the Swiss National Science Foundation and the Kommission zur Förderung der wissenschaftlichen Forschung is gratefully acknowledged.

[1]For recent reviews of spin-polarized probes, see R. J. Celotta and D. T. Pierce, Science **234**, 334 (1986); M. Landolt, Appl. Phys. A **41**, 83 (1986); J. Kirschner, *Polarized Electrons at Surfaces* (Springer-Verlag, Berlin, 1985); C. Rau, J. Magn. Magn. Mater. **30**, 141 (1982); R. Feder, J. Phys. C **14**, 2049 (1981).

[2]G. Binnig, H. Rohrer, Ch. Gerber, and E. Weibel, Phys. Rev. Lett. **49**, 57 (1982).

[3]R. Allenspach and A. Bischof, Appl. Phys. Lett. **54**, 587 (1989).

[4]Y. Manassen, R. J. Hamers, J. E. Demuth, and A. J. Castellano, Jr., Phys. Rev. Lett. **62**, 2531 (1989).

[5]P. M. Tedrow and R. Meservey, Phys. Rev. Lett. **26**, 192 (1971).

[6]M. Julliere, Phys. Lett. **54A**, 225 (1975); S. Maekawa and U. Gäfvert, IEEE Trans. Magn. **18**, 707 (1982); J. C. Slonczewski, J. Phys. (Paris), Colloq. **49**, C8-1629 (1988).

[7]S. Blügel, D. Pescia, and P. H. Dederichs, Phys. Rev. B **39**, 1392 (1989).

[8]R. Wiesendanger, G. Tarrach, D. Bürgler, T. Jung, L. Eng, and H.-J. Güntherodt, in Proceedings of the Eleventh International Vacuum Congress and Seventh International Conference on Solid Surfaces, Cologne, West Germany, 1989 [Vacuum (to be published)]; R. Wiesendanger, D. Bürgler, G. Tarrach, D. Anselmetti, H. R. Hidber, and H.-J. Güntherodt, in *Proceedings of the International Conference on Scanning Tunneling Microscopy, Oarai, Japan, 1989* [J. Vac. Sci. Technol. A **8**, 339 (1990)].

[9]R. Wiesendanger, G. Tarrach, D. Bürgler, and H.-J. Güntherodt, Europhys. Lett. **12**, 57 (1990).

[10]R. Wiesendanger, D. Bürgler, G. Tarrach, and H.-J. Güntherodt, Surf. Sci. (to be published).

[11]K. P. Kämper, W. Schmitt, G. Güntherodt, R. J. Gambino, and R. Ruf, Phys. Rev. Lett. **59**, 2788 (1987).

[12]K. Schwarz, J. Phys. F **16**, L211 (1986).

[13]F. Meier, D. Pescia, and T. Schriber, Phys. Rev. Lett. **48**, 645 (1982).

[14]L. E. Klebanoff, S. W. Robey, G. Liu, and D. A. Shirley, Phys. Rev. B **30**, 1048 (1984); L. E. Klebanoff, R. H. Victora, L. M. Falicov, and D. A. Shirley, Phys. Rev. B **32**, 1997 (1985).

[15]J. H. Coombs and J. B. Pethica, IBM J. Res. Dev. **30**, 455 (1986).

Vacuum tunneling of spin-polarized electrons detected by scanning tunneling microscopy

R. Wiesendanger, D. Bürgler, G. Tarrach, A. Wadas, D. Brodbeck, and H.-J. Güntherodt
University of Basel, Institute of Physics, Klingelbergstrasse 82, CH-4056 Basel, Switzerland

G. Güntherodt
RWTH Aachen, II. Institute of Physics, D-5100 Aachen, Federal Republic Germany

R. J. Gambino and R. Ruf
IBM Thomas J. Watson Research Center, Yorktown Heights, New York 10598

(Received 24 July 1990; accepted 30 November 1990)

We show that the scanning tunneling microscope (STM), operated in ultrahigh vacuum, can be made sensitive to the electron spin and therefore to magnetic structures down to the atomic scale. The experiments were performed with a ferromagnetic CrO_2 tip providing electrons of high spin polarization. As sample, we used a Cr(001) single crystal which offers an ideal magnetic test structure. The experimental results obtained with the ferromagnetic CrO_2 tip characteristically differ from those obtained with a nonmagnetic tungsten tip. We give an expression, relating the local electron spin polarization of the tunneling junction with quantities directly measurable with the STM. We also discuss possible contributions from magnetic dipole and exchange forces as well as the feasibility of magnetic exchange force microscopy.

I. INTRODUCTION

It was already at the First International Conference on Scanning Tunneling Microscopy when "magnetic tunneling" experiments with a scanning tunneling microscope (STM) were mentioned as a promising extension of atomic resolution studies to the field of surface magnetism.[1] In the magnetic version of the force microscope, where the long-range magnetic dipole forces are probed,[2,3] the lateral resolution is limited to some tens of nanometers due to the slow decay of the magnetic dipole forces with increasing tip–surface separation. In contrast, STM involving tunneling of spin-polarized electrons offers the opportunity to probe real-space magnetic structures down to the atomic scale. However, the smallness of the expected change of the current due to tunneling of spin-polarized electrons leads to stringent experimental requirements which have not been met before.

First, a highly stable STM operating in the low 10^{-11} mbar range is necessary since surface magnetism is known to be influenced by only slight surface contamination. Secondly, a source of electrons with high spin polarization (preferably near 100%) is needed to ensure the maximum possible effect. Thirdly, an appropriate magnetic test structure is required.

In the following, we first describe our experimental setup together with our choice of tip and sample (Sec. II). We then present the experimental results (Sec. III) and their interpretation (Sec. IV). Finally, we discuss the possible influence of forces (magnetic dipole and exchange forces) on the experimental results (Sec. V). We also comment on the feasibility of a magnetic exchange force microscope which, in contrast to conventional magnetic force microscopy, would also offer the opportunity to study magnetic structures down to the atomic scale.

II. EXPERIMENT

The tunneling microscope used for the present investigations is part of a multichamber UHV system (NANOLAB) with several surface preparation and analysis facilities which has previously been described in detail.[4,5] All experiments reported here were performed at 1×10^{-11} mbar. The calibration of the STM scanning unit was accomplished by imaging the atomic structure of Si(111) 7×7[6] and Si(001) 2×1[7] surfaces. The noise level of the STM instrument is well below 0.1 Å which was proven by imaging the atomic structure of the hexagonally close-packed Au(111) surface with a measured corrugation of 0.2 Å.[4,5] The quality of STM images obtained with our instrument is also demonstrated by another contribution in these Proceedings.[8]

As source of electrons with a high spin polarization, we have chosen ferromagnetic CrO_2 tips. These CrO_2 tips consist of a 1 μm thick CrO_2 film with in-plane magnetization deposited on Si(111) substrates covered with a TiO_2 nucleation layer. The silicon substrates were cleaved in such a way that tips were obtained. Finally, the substrates were etched back in $HF–HNO_3$ solution leading to overhanging CrO_2 films which can be used as magnetic probes. The films have a large remanent magnetization ($\sim$90% of saturation). Therefore, the tips are likely to be in a single domain, saturated state. It has recently been shown by spin-resolved photoemission on similar CrO_2 films that the spin polarization is nearly 100% for electrons emerging from states with binding energies near 2 eV below the Fermi level.[9] Although the electron spin polarization as measured by spin-resolved photoemission is not necessarily the same as in tunneling experiments, it was hoped that the spin polarization of electrons tunneling out of the occupied states of the CrO_2 tip would be high enough to detect a sign for spin-dependent tunneling.

Magnetic test structures on the atomic scale are offered by antiferromagnets. This choice has two advantages. First, the antiferromagnetic coupling allows the spins to be in opposite directions over interatomic distances which provides the most challenging structure for atomic resolution magnetic microscopies. Secondly, in contrast to ferromagnets, the long-range magnetic dipole field of an antiferromagnet is almost canceled by the alternating spin alignment. This is important for excluding the possible influence of magnetic dipole forces on the experimental results as will be discussed in Sec. V. As an electrically conducting antiferromagnet, we have chosen Cr with bulk bcc structure. The magnetic bulk structure of Cr is well known from neutron scattering experiments and is shown in Fig. 1(a). Depending on the type of surface [e.g., (001), (110) or (111)], different magnetic surface structures of Cr can be studied. Since the CrO_2 tips could not be prepared as sharp as electrochemically etched W tips so far, we did not believe to get in-plane atomic resolution with such tips right at the beginning. However, a high resolution perpendicular to the surface plane can always be expected. Therefore, we have not chosen the Cr(111) surface with in-plane antiferromagnetic structure but the Cr(001) surface which provides a simpler magnetic test structure. In Fig. 1(b) we present the structure of the Cr(001) surface as proposed on the basis of self-consistent total-energy calculations[10] and consistent with experimental results from spin-resolved[11] and angle-resolved photoemission.[12,13] Characteristic for the proposed surface structure of Cr(001) is the occurrence of ferromagnetic terraces which are separated by monatomic steps and alternately magnetized in opposite directions. It is important that the surface Néel temperature of about 800 K for Cr(001)[12] is well above room temperature at which the STM experiments were performed.

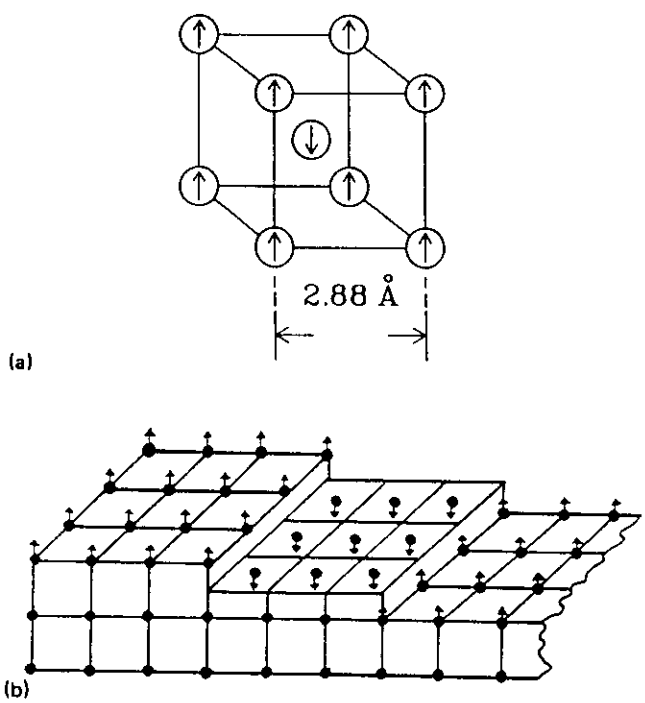

FIG. 1. (a) Spin-lattice of antiferromagnetic Cr. (b) Alternately magnetized terraces of a Cr(001) surface. The terraces are separated by monatomic steps of 0.144 nm height (from Ref. 10).

III. RESULTS

The mechanically and electrolytically polished Cr(001) surface was prepared *in situ* over a time period of several months by cycles of Ar^+ ion etching and annealing. A $p(1\times1)$ low-energy electron diffraction pattern was obtained, characteristic of a clean Cr(001) surface.[12,13] Only small traces of oxygen and nitrogen were finally detected by x-ray photoelectron spectroscopy.

Topographic STM studies performed with a nonmagnetic, electrochemically etched W tip support the microscopic model of terraces separated predominantly by monatomic steps as shown in Fig. 2. The shape of the terraces as well as their average width depend on the surface preparation conditions. However, the preferred occurrence of monatomic steps was found to be independent of the surface preparation and the experimentally determined value of the monatomic step height (1.49 ± 0.08 Å) is in good agreement with half of the cubic unit cell height of bcc Cr (1.44 Å).

The terrace structure of the Cr(001) surface also appears in STM images obtained with a ferromagnetic CrO_2 tip as shown in Fig. 3(a). However, several differences between W and CrO_2 tips became evident. First, a positive sample bias voltage of at least 2 V had to be applied in the STM experiments with the CrO_2 tip in order to get a stable tunneling current of 1 nA. The I–V characteristics showed the typical appearance of semiconductor–vacuum–metal tunneling. This observation is consistent with the low intensity in the photoemission spectra of CrO_2 near the Fermi level.[9] Therefore, the possible explanation of the high spin polarization of electrons from CrO_2 as being a half-metallic ferromagnet[14] is questionable. It now seems more likely that CrO_2 must be regarded as a semiconductor-like ferromagnet.

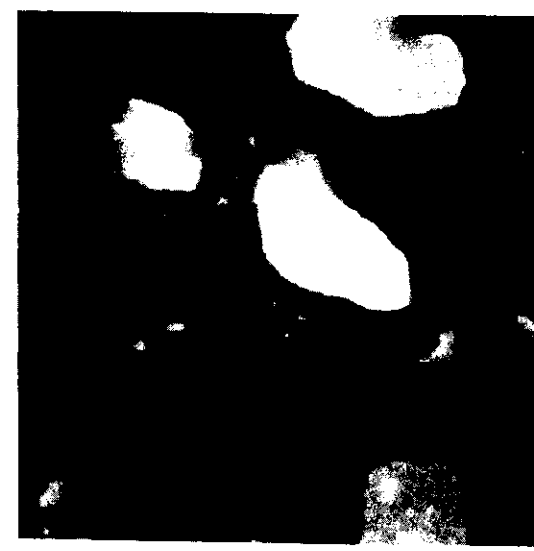

FIG. 2. Overview STM image (128×128 nm^2) of the Cr(001) surface obtained with a tungsten tip at a constant tunneling current. The terraces, which are predominantly separated by monatomic steps, appear in different grey levels according to their relative height. The tunneling parameters were $I = 1$ nA and $U = +0.05$ V.

(a)

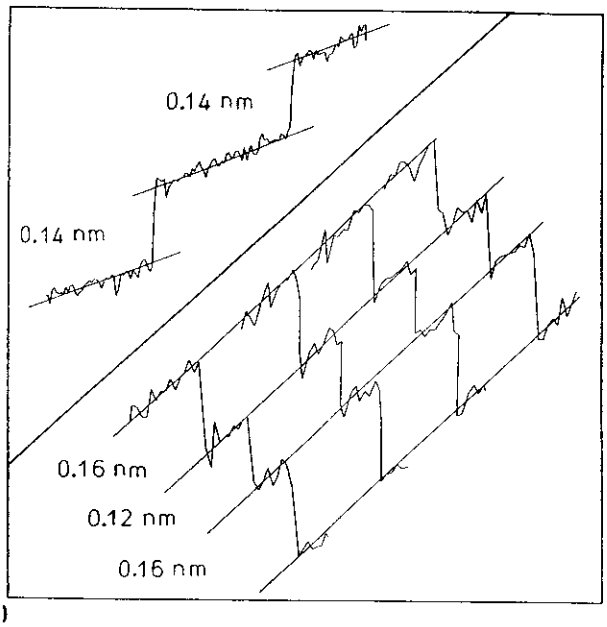

(b)

FIG. 3. (a) Top-view STM image (32×32 nm^2) of the Cr(001) surface obtained with a CrO_2 tip at a constant tunneling current. Again, terraces separated by monatomic steps can be seen which show up in different grey levels. The tunneling parameters were $I = 1$ nA and $U = +2.5$ V. (b) Arbitrarily chosen (not successive) single line scans over the same three monatomic steps taken from the STM image of (a), which was obtained with a CrO_2 tip. The same alternation of the step-height values (0.16, 0.12, and again 0.16 nm) in all single line scans is evident. The line scans are 22 nm long. Inset: For comparison, a single line scan over two monatomic steps taken from the STM image of Fig. 2, which was obtained with a tungsten tip. In this case, the measured step-height value is constant and corresponds to the topographic monatomic step height. This line scan is 70 nm long.

Second, while scanning over the alternately magnetized terraces, a characteristic periodic alternation of the measured monatomic step-height values around the mean value of 1.44 Å can be observed with a ferromagnetic CrO_2 tip which has never been found with a nonmagnetic W tip [Fig. 3(b)]. This periodic alternation of the measured monatomic step-height values cannot be explained by a statistical fluctuation of the measured step-height values since the same alternation (including the sequence of larger and smaller measured step-height values as well as the amount of the deviation from the mean monatomic step-height value) is reproducibly observed in different line scans which can be regarded as independent measurements. The reproducibility is not only given within a single STM image but also for successive STM images of the same surface area. In Fig. 4(a) we present another STM image obtained at the same location as the image presented in Fig. 3(a). Note that the imaged surface areas in Figs. 3(a) and 4(a) have a different size. If we now analyze the measured step-height values for the same three monatomic surface steps, we find the identical periodic alternation (including the sequence as well as the amount of deviation) of the measured step-height values.

In the following Sec. IV, we will give an explanation for this observed periodic alternation of the measured step-height values based on vacuum tunneling of spin-polarized electrons from the ferromagnetic CrO_2 tip into the Cr(001)

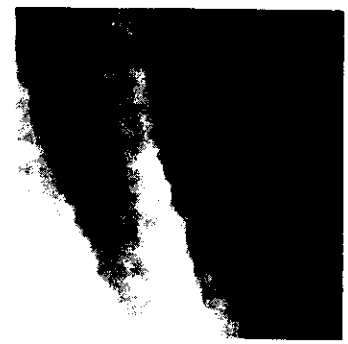

(a)

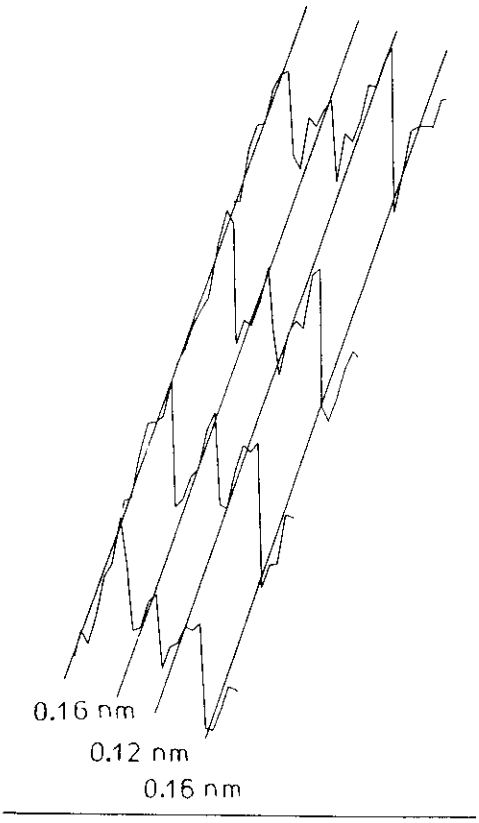

(b)

FIG. 4. (a) Another STM image (50×50 nm^2) of the Cr(001) surface obtained with the CrO_2 tip at the same location as for the image presented in Fig. 3(a). The tunneling parameters were the same as for Fig. 3(a). (b) The identical periodic alternation of the measured step-height values is found in the STM image of (a) for the same three monatomic surface steps which have already been analyzed in Fig. 3(b).

sample. In Sec. V, we will show that alternative explanations based on the influence of magnetic forces can be ruled out.

IV. INTERPRETATION

Slonczewski[15,16] has already shown that the conductance G of a tunneling junction consisting of two ferromagnets is dependent on the relative orientation of the magnetization vectors within the two electrodes. A magnetic valve effect is predicted consisting of an increased conductance $G = G_0(1 + P)$ in the case of parallel magnetization vectors and a reduced conductance $G = G_0(1 - P)$ in the case of antiparallel magnetization vectors. (We denote P as the effective polarization of the magnet–barrier–magnet junction and G_0 as the conductance of the tunneling junction without considering spin-dependent tunneling.) In our experiment, the tip magnetization vector is known to lie in the plane of the CrO_2 film. Within this plane, the shape anisotropy of the tip leads to a preferred direction of the magnetization along the tip axis. Therefore, the tip magnetization vector is perpendicular to the sample surface plane. Assume, as in Fig. 5, that such a tip is scanning over the alternately magnetized terraces of the Cr(001) surface. According to the theory of Slonczewski, the tunneling current would alternately increase and decrease while scanning over the different terraces at a constant height s_0. However, since we are operating our STM at constant tunneling current, the tip has to withdraw from or come closer to the surface depending on the magnetization direction of the terraces. This automatically leads to a periodic alternation of the measured monatomic step-height values between larger and smaller values as observed experimentally. One can easily show that the relationship between the effective polarization P of the magnet–barrier–magnet junction and the deviation Δs of the larger and smaller measured step-height values from the topographic step-height value is given by[17]

$$P = \frac{\exp(A\sqrt{\phi}\Delta s) - 1}{\exp(A\sqrt{\phi}\Delta s) + 1},$$

where ϕ is the mean local tunneling barrier height and $A \approx 1$ eV$^{-1/2}$ Å^{-1}. Since Δs and ϕ can directly be measured by STM, the local effective spin polarization of the tunneling junction can be determined. From Figs. 3(b) and 4(b) we derive $\Delta s = (0.2 \pm 0.1)$ Å. We also measured ϕ from the slope of local log I–s characteristics and obtained values around (4 ± 0.5) eV. Therefore, we derive a value for P of about $(20 \pm 10)\%$.

Assuming a spin-dependent tunneling probability $T(s_1, s_2) = \delta_{s_1,s_2}$, where s_1 and s_2 denote the spin directions of the initial and final state, we calculated P based on published density-of-states calculations.[14,18] Generally, P cannot be expressed as a product of the spin polarizations of the two independent electrodes. The value of P turns out to be characteristic for a special tunneling junction at a particular bias voltage. Varying the bias voltage can change the value and even the sign of P as shown in Fig. 6. The experimentally obtained value of P at a sample bias voltage of $+2.5$ V is in good agreement with the result of the calculation. Future bias and distance dependent measurements of P as well as spatially resolved measurements of P are particularly promising.

V. FORCES

One might argue that the influence of magnetic forces could also lead to the observed alternation of the monatomic step-height values when measuring with a ferromagnetic tip. We first consider magnetic dipole forces. In Fig. 7, we present a calculation of the z component of this force for a tip magnetized along the tip axis (z direction), while the tip is scanned over alternately magnetized surface regions. We assumed a magnetization field of 500 Oe for the tip and a width of the homogeneously magnetized surface regions of 10 nm. From experiments observing the transition from the tunneling regime to the formation of point contact, we know the distance between the CrO_2 tip and the Cr(001) surface for a tunneling current of 1 nA and a sample bias voltage of 2.5 V. This distance d was determined to be about 5 Å. The calculation of the magnetic dipole force was performed for $d_1 = 5$ Å and $d_2 = 3$ Å. The value of this force came out to be of the order of 10^{-11} N. However, the force is largely overestimated in our calculations since we assumed the shape of the tip

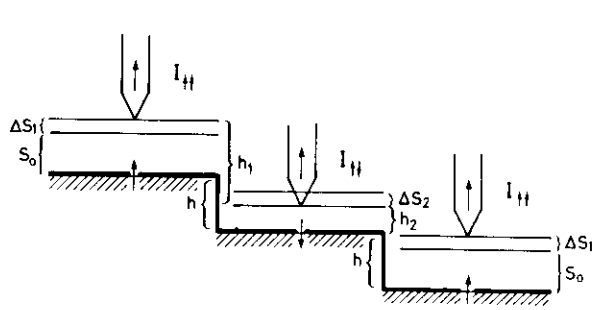

FIG. 5. With a ferromagnetic tip scanned over alternately magnetized terraces, the measured step-height values are not identical with the topographic step-height h but alternate between $h_1 = h + \Delta s_1 + \Delta s_2$ and $h_2 = h - \Delta s_1 - \Delta s_2$ due to an additional contribution from spin-dependent tunneling.

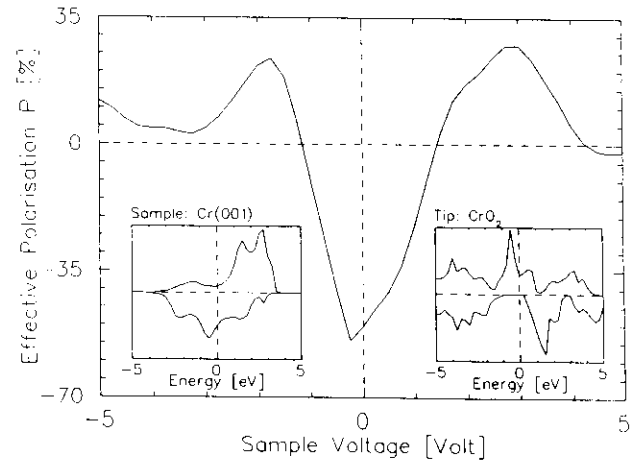

FIG. 6. Effective spin polarization of the CrO_2–vacuum–Cr(001) junction as a function of sample bias voltage. The insets show the spin-up (upper part) and the spin-down (lower part) density-of-states of CrO_2 and the Cr(001) surface.

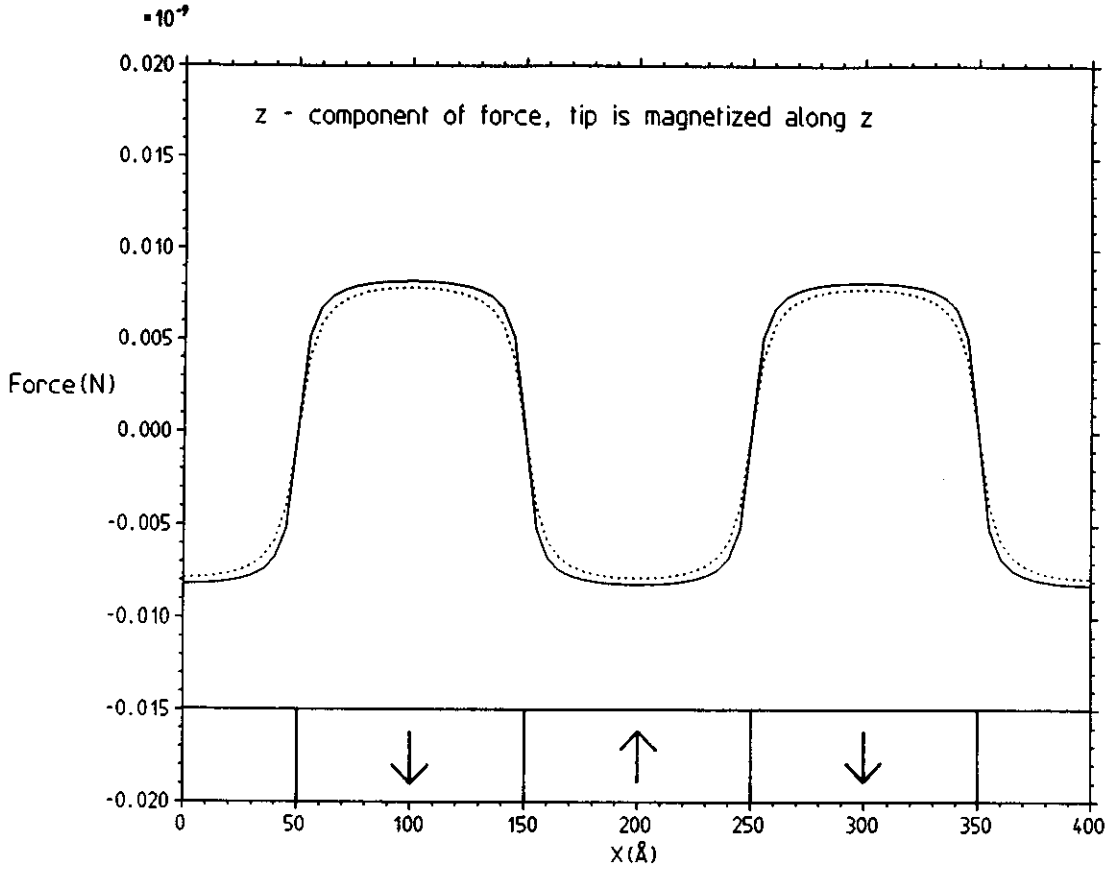

FIG. 7. Magnetic dipole force acting on a ferromagnetic tip while scanning over alternately magnetized surface regions in a distance of 3 Å (solid line) and 5 Å (dotted line). A magnetization of 500 Oe with direction along the tip axis was assumed.

to be a truncated pyramid (height: 10 μm, base areas: 0.16 and 243.36 μm^2), whereas in reality, the CrO_2 tip consisted of a thin film of 1 μm thickness overhanging for about 10 μm over the Si(111) substrate. Estimates of the spring constant of the overhanging CrO_2 film yield values of at least 500 N m^{-1}. This spring constant is, however, effective only for forces acting parallel to the surface plane. Even if we calculate the resulting deflections by taking this spring constant of 500 N m^{-1} and forces of the order of 10^{-11} N, we obtain values of the order of 10^{-4} Å. This is far below the deviation of the measured step-height values from the topographic step height which can be as large as 0.2 Å [Figs. 3(b) and 4(b)]. In conclusion, magnetic dipole forces acting between the ferromagnetic CrO_2 tip and the antiferromagnetic Cr sample can be neglected in our experiment.

We finally consider the possible influence of magnetic exchange forces. We have not exactly calculated these forces for the STM-type geometry. However, we have estimated the magnetic exchange force per unit area as a function of the distance between the two electrodes according to a recent theoretical work by Slonczewski.[16] The results are presented in Fig. 8. For a tip–surface distance of 5 Å, we obtain a force of about 5×10^{-14} N Å^{-2}. From the sharpness of the monatomic steps imaged with the CrO_2 tip, we estimate the effective radius of this tip not to be larger than 20 Å. Only this effective tip radius is important when considering the short-range exchange forces in contrast to the long-range dipole forces. The exchange force is therefore of the order of 10^{-11}–10^{-10} N. Again, the derived deflections, even by assuming an effective spring constant of 500 N m^{-1}, are negligible. The situation would, however, change if, instead of a CrO_2 tip, a cantilever beam with a spring constant of about 1 N m^{-1} or even less is used in an AFM-type experiment.

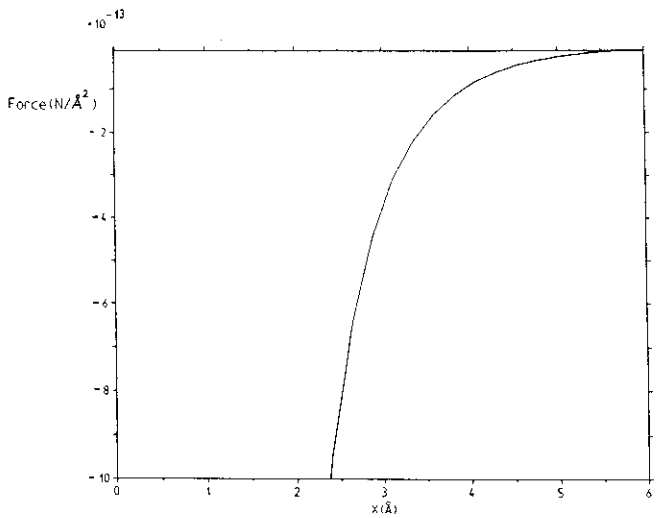

FIG. 8. Magnetic exchange force per Å^2 as a function of the separation between the two electrodes.

Magnetic exchange forces should then easily be detectable at smaller tip–surface separations (less than 5 Å) where these forces strongly increase (Fig. 8). To exclude a dominant contribution from magnetic dipole forces, either the tip or the sample has to be an antiferromagnet. With such a magnetic exchange force microscope, high spatial resolution can be expected due to the large force gradient.

VI. CONCLUSIONS

We have presented STM experiments involving a ferromagnetic CrO_2 tip and a Cr(001) surface. A characteristic periodic alternation of the measured monatomic step-height values can be observed which has never been found when measuring with a nonmagnetic W tip. We can explain these experimental results only by assuming vacuum tunneling of spin-polarized electrons from the CrO_2 tip into the Cr(001) sample. Estimates of magnetic forces acting in our experiment show that these forces can be neglected. However, the calculations indicate that magnetic exchange force microscopy involving at least one antiferromagnetic electrode and tip–surface distances of less than 5 Å should be feasible.

ACKNOWLEDGMENTS

We would like to thank Professor A. Hubert for stimulating discussions as well as for electropolishing the Cr(001) single crystal. We also thank H. Breitenstein, H. R. Hidber, P. Reimann, R. Schnyder, and A. Tonin for their technical help. Financial support from the Swiss National Science Foundation and the Kommission zur Förderung der wissenschaftlichen Forschung is gratefully acknowledged.

[1] G. Binnig, invited talk held at the 1st Int. Conf. STM'86, Santiago de Compostela, Spain (unpublished).
[2] Y. Martin, D. Rugar, and H. K. Wickramasinghe, Appl. Phys. Lett. **50**, 1455 (1987).
[3] J. J. Saenz, N. Garcia, P. Grütter, E. Meyer, H. Heinzelmann, R. Wiesendanger, L. Rosenthaler, H. R. Hidber, and H.-J. Güntherodt, J. Appl. Phys. **62**, 4293 (1987).
[4] R. Wiesendanger, D. Bürgler, G. Tarrach, D. Anselmetti, H. R. Hidber, and H.-J. Güntherodt, J. Vac. Sci. Technol. A **8**, 339 (1990).
[5] R. Wiesendanger, G. Tarrach, D. Bürgler, T. Jung, L. Eng, and H.-J. Güntherodt, Vacuum **41**, 386 (1990).
[6] R. Wiesendanger, G. Tarrach, D. Bürgler, and H.-J. Güntherodt, Europhys. Lett. **12**, 57 (1990).
[7] R. Wiesendanger, D. Bürgler, G. Tarrach, and H.-J. Güntherodt, Surf. Sci. **232**, 1 (1990).
[8] G. Tarrach, R. Wiesendanger, D. Bürgler, L. Scandella, and H.-J. Güntherodt J. Vac. Sci. Technol. B **9**, xxxx (1991).
[9] K. P. Kämper, W. Schmitt, G. Güntherodt, R. J. Gambino, and R. Ruf, Phys. Rev. Lett. **59**, 2788 (1987).
[10] S. Blügel, D. Pescia, and P. H. Dederichs, Phys. Rev. B **39**, 1392 (1989).
[11] F. Meier, D. Pescia, and T. Schriber, Phys. Rev. Lett. **48**, 645 (1982).
[12] L. E. Klebanoff, S. W. Robey, G. Liu, and D. A. Shirley, Phys. Rev. B **30**, 1048 (1984).
[13] L. E. Klebanoff, R. H. Victoria, L. M. Falicov, and D. A. Shirley, Phys. Rev. B **32**, 1997 (1985).
[14] K. Schwarz, J. Phys. F **16**, L211 (1986).
[15] J. C. Slonczewski, J. Phys. C **8**, 1629 (1988).
[16] J. C. Slonczewski, Phys. Rev. B **39**, 6995 (1989).
[17] R. Wiesendanger, H.-J. Güntherodt, G. Güntherodt, R. J. Gambino, and R. Ruf, Phys. Rev. Lett. **65**, 247 (1990).
[18] G. Allan, Surf. Sci. **74**, 79 (1978).